Symplectic Maps for Diverted Plasmas

Iberê Luiz Caldas, Bruno F. Bartoloni, David Ciro, Geraldo Roberson, Adriane B. Schelin, Tiago Kroetz, Marisa Roberto, Ricardo Luiz Viana, Kelly Cristiane Iarosz, Antonio Marcos Batista, and Philip J. Morrison

***Abstract*— Nowadays, divertors are used in the main tokamaks to control the magnetic field and to improve the plasma confinement. In this paper, we present analytical symplectic maps describing Poincaré maps of the magnetic field lines in confined plasmas with a single-null poloidal divertor. Initially, we present a divertor map and the tokamap for a diverted configuration. We also introduce the Ullmann map for a diverted plasma, whose control parameters are determined from tokamak experiments. Finally, an explicit, area-preserving, and integrable magnetic field line map for a single-null divertor tokamak is obtained using a trajectory integration method to represent toroidal equilibrium magnetic surfaces. In this method, we also give examples of onset of chaotic field lines at the plasma edge due to resonant perturbations.**

***Index Terms*— Divertor, magnetic surfaces, symplectic map.**

I. Introduction

TOKAMAKS are the most promising devices to confine fusion plasmas [1], [2]. The plasma confinement depends on the magnetic field, which determines the particle transport [3]. To the leading order approximation, the charged particles follow the magnetic field lines [2], [3]. Thus, the particle transport can be controlled by properly modifying the magnetic field as a result of electrical currents in external coils and also by installing poloidal divertors [1], [4]. Such divertors are used to control the plasma impurity content [5], [6] and have a special magnetic configuration created by electric currents in external coils, such that the field lines have escape channels, through which plasma particles can be diverted out of the tokamak wall and redirected to divertor plates.

Divertors are essential components in modern tokamaks, such as International Thermonuclear Experimental Reactor (ITER) [1], [7]. The overlap of the magnetic fields created by the divertor with the magnetic field of the plasma creates a hyperbolic fixed point where the poloidal magnetic field is null. The hyperbolic point is in the separatrix, the invariant line separating the plasma, with stable and unstable manifolds [8], [9]. Outside the separatrix, the magnetic field lines intersect the collector plates [1].

The tokamak map trajectories can be obtained by directly integrating the field line differential equations, but the integration requires a time-consuming calculation, which may not be appropriate for studying long term of the field behavior. Therefore, approximated maps have to be considered if one wants to have the advantage of much shorter computation times [3], [10], [11]. Analytical tokamak maps can be derived from physical models and mathematical approximations applied to the field line equations or even can be *ad hoc* maps to obtain a qualitative or quantitative description of the physical situation that they describe [11]–[13].

Magnetic field lines are, in general, orbits of Hamiltonian systems of one-and-a-half degrees of freedom with a timelike periodic coordinate. Consequently, the field line configuration can be represented in Poincaré sections at a fixed toroidal angle, equivalent to 2-D area-preserving maps [3], [10], [11]. Thus, we can use such maps to qualitatively represent the magnetic configurations of tokamak plasmas [14]. In this paper, we present maps proposed to investigate the fundamental features of the magnetic field line dynamics in tokamaks with the divertor. We introduce new versions of the tokamap and the Ullmann map for tokamaks with the divertor and review the divertor map and an integrable map for an equilibrium divertor configuration in toroidal geometry.

This paper is organized as follows. In Section II, we show the tokamak divertors. In Section III, we introduce three symplectic maps: the divertor map, the tokamap for divertor configuration, and the Ullmann map for the divertor. We also give examples of these maps to show their dynamical characteristics. In Section IV, we introduce an integrable map to simulate toroidal magnetic surfaces modified by a divertor. Section V contains the conclusions.

II. Divertor

In tokamaks, a material limiter separates the plasma column from the wall. However, to improve the plasma isolation and eliminate impurities, divertors have been used in several

Manuscript received October 26, 2017; revised January 8, 2018; accepted January 18, 2018. This work was supported in part by the National Council for Scientific and Technological Development, Brazil, under Grant 870198/1997-1 and Grant 830577/1999-8 and in part by the São Paulo Research Foundation under Grant 2012/18073-1, Grant 2015/07311-7, and Grant 2011/19296-1. The work of P. J. Morrison was supported by the U.S. Department of Energy Contract under Grant DE-FG05-80ET-53088. The review of this paper was arranged by Senior Editor S. J. Gitomer. *(Corresponding author: Kelly Cristiane Iarosz.)*

I. L. Caldas and K. C. Iarosz are with the Institute of Physics, University of São Paulo, 05508-090 São Paulo, Brazil (e-mail: ibere@if.usp.br; kiarosz@gmail.com).

B. F. Bartoloni is with the Departamento de Ensino Geral, Faculdade de Tecnologia de São Paulo, 01124-060 São Paulo, Brazil.

D. Ciro and R. L. Viana are with the Department of Physics, Federal University of Paraná, 81531-980 Curitiba, Brazil.

G. Roberson and M. Roberto are with the Aeronautics Institute of Technology, CTA, 12228-900 São José dos Campos, Brazil.

A. B. Schelin is with the Institute of Physics, University of Brasília, 70919-970 Brasília, Brazil.

T. Kroetz is with the Department of Mathematics, Federal Technological University of Paraná, 85503-390 Pato Branco, Brazil.

A. M. Batista is with the Department of Mathematics and Statistics, State University of Ponta Grossa, 84030-900 Ponta Grossa, Brazil.

P. J. Morrison is with the Institute for Fusion Studies, The University of Texas at Austin, Austin, TX 78712-0262 USA.

Color versions of one or more of the figures in this paper are available online at http://ieeexplore.ieee.org.

Digital Object Identifier 10.1109/TPS.2018.2797120

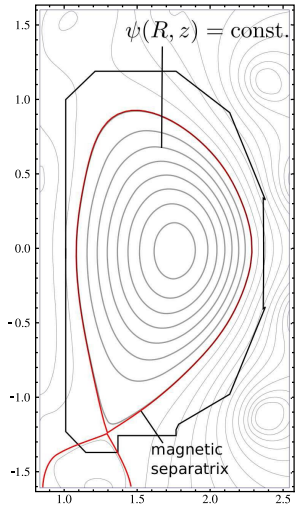

Fig. 1. (Color online) Schematic view of a tokamak divertor equilibrium configuration with intersection of invariant magnetic surfaces on a plane determined by a specific toroidal angle. The red line indicates the magnetic separatrix, while the contours are magnetic surfaces.

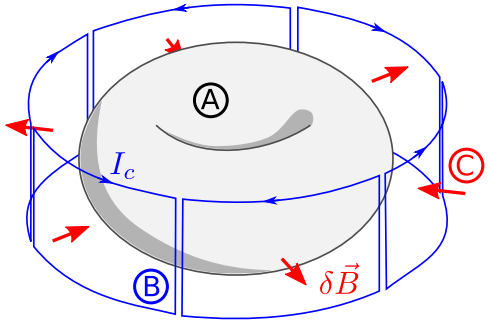

Fig. 2. (Color online) Schematic view of a tokamak vacuum chamber (A) and the external coils (B), responsible for the resonant magnetic field (C). Blue lines indicate the perturbing external currents, and the red vectors indicate the nonaxisymmetric field perturbation.

modern tokamaks and will be used in ITER [7]. Divertors consist of conductors arranged externally that carry specific electric currents to create X-point (or hyperbolic fixed point), where the poloidal magnetic field is null, due to the overlap of the magnetic fields of the conductors with the magnetic field of the plasma.

In Fig. 1, we present an example of the magnetic surfaces in a tokamak with the divertor. In Fig. 1, the separatrix in red line, with one hyperbolic point, separates the internal toroidal magnetic surfaces with quasi-periodic lines of the external surfaces with open field lines. Moreover, the X-point arises from a separatrix with two manifolds, one stable and the other unstable.

Several tokamaks with divertors have nonaxisymmetric resonant perturbation coils designed specifically to modify the plasma magnetic field [1], [2]. One of the actions of the resonant perturbations created by these coils is to create chaotic magnetic field layers in the peripheral region of the plasma column [7], [11], [13].

In Fig. 2, we show an example of this kind of coils arranged around a tokamak chamber, similar to the coils used

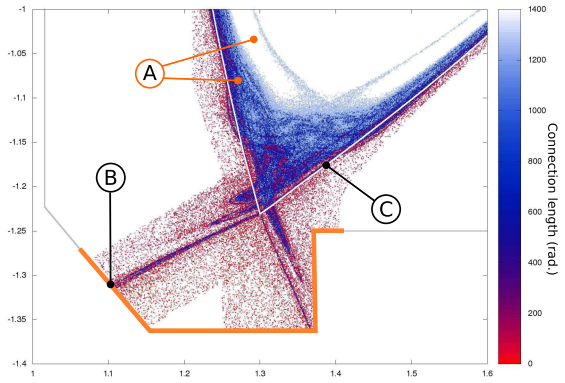

Fig. 3. (Color online) Detail of the Poincaré map of the perturbed field lines in the magnetic saddle region. The magnetic perturbation leads to the formation of a peripheral chaotic layer and magnetic islands (A). Chaotic field lines now cross the symmetric separatrix (C), and the open field lines intersect the tokamak chamber (B) in asymmetric patterns controlled by the invariant manifolds of the saddle.

in DIII-D tokamak [15]. To show how the tokamak equilibrium is perturbed by the coils in Fig. 2, we present in Fig. 3, the transversal cross section of the diverted tokamak magnetic field lines for a set of control parameters commonly found in tokamak discharges [15], [16]. In Fig. 3, we can see chaotic lines and magnetic islands around the divertor hyperbolic point, the separatrix of the unperturbed diverted field, and the divertor plates where the chaotic lines intersect the tokamak chamber.

The chaotic layer at the plasma edge affects the plasma confinement [17] and can be controlled by the perturbation introduced by the divertor [7]. The chaotic layer in this region is mainly determined by the manifolds from the hyperbolic point [18].

III. Sympletic Maps

Symplectic maps have been commonly used in physics to describe Poincaré sections of dynamical systems [19]–[21]. In plasma physics, a pioneer symplectic map to describe particle orbits for stellarators was introduced in [22]. After that, symplectic maps have been used to investigate particle transport in magnetically confined plasmas [23]–[25]. Symplectic maps have also been introduced to investigate the chaotic field lines in tokamaks. The first one was the Martin–Taylor map introduced to describe the perturbation created by the ergodic magnetic limiter in tokamaks [26].

In this section, we present symplectic maps to describe the diverted magnetic field lines in tokamaks: the divertor map introduced in [27] and the new versions of the tokamap [28] and Ullmann's map [29] for divertors. These maps are nonintegrable and describe plasma equilibrium with chaotic layers, around the hyperbolic point, due to resonant perturbations.

A. Divertor Map

The first divertor map has been presented as the simplest model for the magnetic configuration of a tokamak equipped with a divertor. The map simulates Poincaré sections of field lines [27].

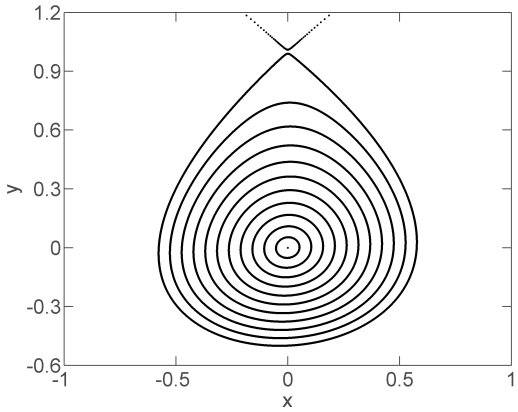

Fig. 4. Poincaré map of the divertor map for $k = 0.6$, depicting the stable fixed point at $(0, 0)$ and some invariant curves. Closed invariant lines are separated from open lines (not shown) by the separatrix, which includes the hyperbolic point at $(0, 1)$.

The divertor map introduced in [27] is

$$\begin{aligned} x_{n+1} &= x_n - k y_n (1 - y_n) \\ y_{n+1} &= y_n + k x_{n+1} \end{aligned} \tag{1}$$

where (x_n, y_n) are the rectangular coordinates on the poloidal surface of the section, and the control parameter k determines both the safety factor and the strength of toroidal asymmetries in the magnetic field. In this map, the equilibrium and perturbation expressions cannot be separated, and consequently, we cannot describe the equilibrium without perturbation. For the small values of the control parameter k, the map shows the formation of a thin chaotic layer in the separatrix region, whose chaotic orbits eventually reach the plates, which are set in the numerical simulations at $y_{\text{plate}} = 1$. One example is in Fig. 4 for $k = 0.6$.

B. Tokamap for Diverted Plasmas

The tokamap has been introduced to describe field lines of a tokamak equilibrium modified by a resonant perturbation. There are several versions of this map to account for different equilibria and perturbations. Here, we consider the following version of the map for tokamak plasmas [28]:

$$\begin{aligned} \psi_{k+1} &= \psi_k - \frac{L}{2\pi} \frac{\psi_{k+1}}{1 + \psi_{k+1}} \sin(2\pi\theta_k) \\ \theta_{k+1} &= \theta_k + \frac{1}{q(\psi_{k+1})} - \frac{L}{2\pi} \frac{1}{(1 + \psi_{k+1})^2} \cos(2\pi\theta_k) \end{aligned} \tag{2}$$

where L is a control parameter that simulates the resonant perturbation amplitude and q is the safety factor that characterizes the tokamak equilibrium.

We use rectangular coordinates $x = (\theta/2\pi)$ and $y = 1 - (\Psi/\Psi_a)$, where $\Psi_a = \Psi$ at the plasma edge. We choose a safety profile divergent near the plasma edge ($x = 1$ at the plasma edge and $x = 0$ at the plasma center). The considered profile is shown in Fig. 5. In Fig. 6, we show invariant and chaotic lines, around the hyperbolic point, for the control parameter $L = 0.1$. The observed chaotic layer appears in the resonant region.

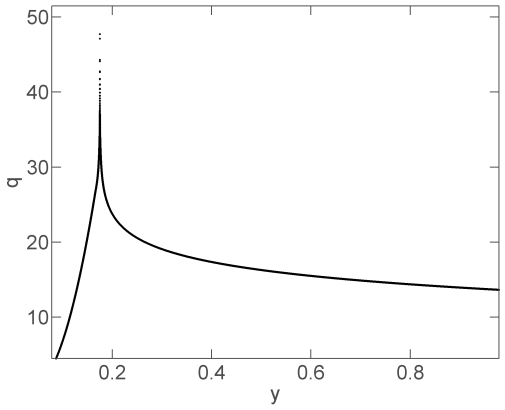

Fig. 5. Safety factor profile considered for the tokamap to obtain Fig. 6. The coordinate y corresponds to the radial coordinate used in large aspect-ratio tokamaks.

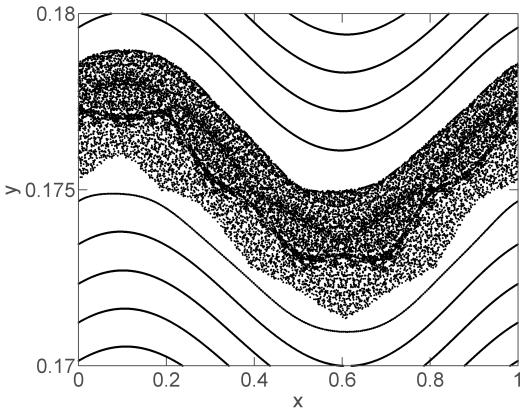

Fig. 6. Invariant magnetic surfaces and chaotic field lines obtained from the tokamap for $L = 0.1$.

C. Ullmann Map for Diverted Plasma

A special set of coils, known as the ergodic limiter, have been proposed to create a chaotic layer at the tokamak plasma edge in order to separate the plasma from the wall [4]. Since then, different kinds of limiters were installed in tokamaks to control the plasma confinement [12], [13], [30].

In [29], a symplectic map was proposed to describe tokamak field lines perturbed by an ergodic limiter. The map is valid for large aspect-ratio tokamaks with toroidal correction. In this approximation, the toroidal coordinate is related to z. In the model, the topology of the magnetic field lines is described by a Poincaré map in the section $z =$ constant, with variables r_n *and* Θ_n denoting the coordinates of the nth intersection of the field line on the considered section [12], [29].

The analytical expressions for the Poincaré map is obtained, for the equilibrium with toroidal correction, by the generating function

$$\begin{aligned} G_{\text{TO}}(r_{n+1}, \theta_n) &= G_{\text{cil}}(r_{n+1}, \theta_n) \\ &\quad + \sum_{l=1}^{\infty} a_l \left(\frac{r_{n+1}}{R_0} \right)^l \cos(l\theta_n) \end{aligned} \tag{3}$$

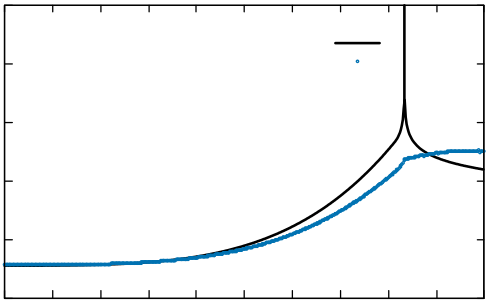

Fig. 7. Analytical safety factor profile, with a divergence near the plasma edge, and the safety factor profile calculated numerically, for fixed θ. The coordinate r is normalized to a (plasma radius).

and the following relations:

$$r_n = \frac{\partial G_{\mathrm{TO}}(r_{n+1}, \theta_n)}{\partial \theta_n} \tag{4}$$

$$\theta_{n+1} = \frac{\partial G_{\mathrm{TO}}(r_{n+1}, \theta_n)}{\partial r_{n+1}} \tag{5}$$

where G_{cil} is the generating function corresponding to the cylindrical equilibrium. From (4) and (5), we obtain the map expressions

$$r_{n+1} = \frac{r_n}{1 - a_1 \sin\theta_n} \tag{6}$$

$$\theta_{n+1} = \theta_n + \frac{2\pi}{q(r_{n+1})} + a_1 \cos\theta_n \tag{7}$$

where a_1 is small and determined by the inverse of the tokamap aspect ratio, and $q(r)$ is the safety factor profile. The toroidal correction introduces a poloidal angle θ dependence on the map. Such correction, considered in the model, takes into account the outward magnetic surface displacement, a characteristic of tokamak equilibrium in toroidal geometry. The constant $a_1 = -0.04$ was fit to reproduce the observed tokamak magnetic surface displacements [29]. Since the map is derived from a generating function, interpreted as a canonical transformation between the previous and the next coordinates, the Jacobian for this map is unitary, and consequently, the map is symplectic [12], [29].

We consider the Ullmann map with the safety factor profile used in the tokamap without the toroidal corrections, i.e., $a_1 = 0$, which is integrable. This is compared with the safety factor profile of the nonintegrable case with toroidal correction $a_1 = -0.04$. The latter must be obtained numerically by inverting the rotation number of an appropriate collection of initial conditions. This is accomplished using the relation

$$q = \frac{1}{l} \to q \equiv \lim_{k\to\infty} \frac{2\pi k}{\sum_{j=0}^{k}(\theta_{j+1} - \theta_j)}. \tag{8}$$

In Fig. 7, we have the analytical safety factor profile obtained from this definition and, for initial conditions with fixed θ, the modified safety factor calculated numerically for 100 values of r between 0 and 1. We see in Fig. 7 the difference between the original profile inserted in (7) and the one calculated, considering the toroidal correction, by applying (8). The profiles are the same in the plasma center and differ at the plasma edge. As shown in [12] and [29], we can add another symplectic map as an external perturbation to obtain a chaotic layer on the resonant region.

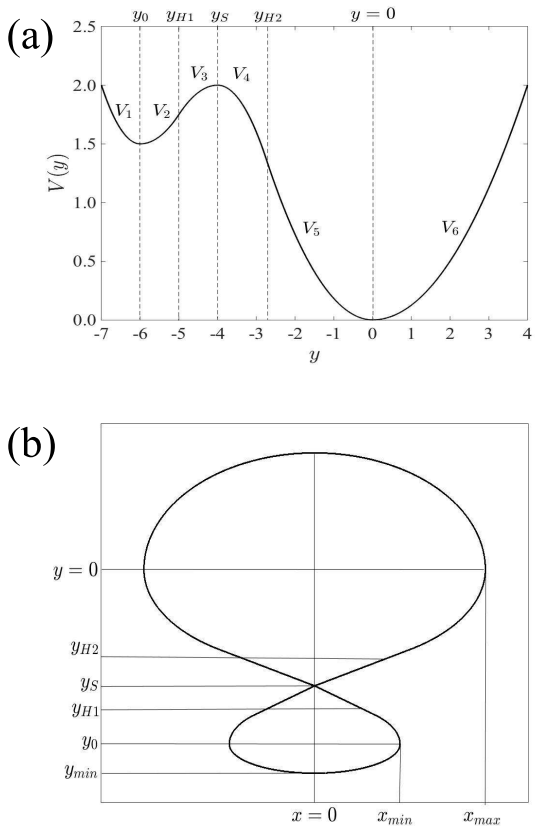

Fig. 8. (a) Potential used to obtain the magnetic surfaces. (b) Schematic of a separatrix in rectangular coordinates indicating the meaning of each geometric parameter related to $V(y)$ for the normalized geometric parameters $x_{\max} = -2$, $x_{\min} = -1$, $y_{\min} = 7$, $y_{\max} = 4$, $y_{H1} = 5$, $y_{H2} = 2.75$, $y_S = 4$, and $y_0 = 6$.

IV. Integrable Map for Toroidal Magnetic Surfaces

In this section, we introduce a procedure to obtain an integrable map simulating a plasma equilibrium for a diverted tokamak [31]–[33].

To obtain the desired map, it is necessary, initially, to find a potential $V(y)$ that produces a topology with an X-point, with Hamiltonian ψ given by

$$\psi = \frac{x^2}{2} + V(y). \tag{9}$$

In the plasma map, this Hamiltonian will be the flux function. We choose a double-well shaped potential to create curves in phase space that exhibit two closed regions delimited by a separatrix between them with an X-point. The expression for $V(y)$ with the desired properties will be written as a set of six parabolas, indicated in Fig. 8(a), joined smoothly the connection points. In Fig. 8(a), each portion between two dashed lines has its own parameters, and then, there are six different parabolas joining smoothly at the dashed lines. Fig. 8(a) shows the chosen potential profile used in this paper [31]. A higher number of parabolas could be used to

adapt the plasma shape to a desired boundary. Three parabolas are the minimum to reproduce the divertor configuration with one hyperbolic and two elliptic points. The position $y = 0$ corresponds to the plasma center. In Fig. 8(b), we present the separatrix for the orbits obtained for the chosen potential of Fig. 8(a). This separatrix determines, in the map, the last closed magnetic surfaces inside the plasma.

We choose an analytical expression for the potential represented in Fig. 8(a). For this potential, the trajectory corresponding to the separatrix is shown in Fig. 8(b), for ITER parameters.

The next step is to solve Hamilton's equations to get x and y in terms of their initial conditions (x_0, y_0) and time t

$$\frac{dx}{dt} = -\frac{\partial \psi}{\partial y} \tag{10}$$

$$\frac{dy}{dt} = \frac{\partial \psi}{\partial x}. \tag{11}$$

The continuous equations are transformed into a discrete map, where the continuous-time parameter t is turned into a discrete-time step Δ

$$x(x_0, y_0, t) = x_{n+1}(x_n, y_n, \Delta) \tag{12}$$

$$y(x_0, y_0, t) = y_{n+1}(x_n, y_n, \Delta). \tag{13}$$

To obtain the magnetic surfaces, we choose Δ given by the inverse of the safety factor

$$\Delta = \frac{T(\psi)}{q(\psi)} \tag{14}$$

where $T(\psi)$ is the rotation period of the invariant curves associated with the continuous system and $q(\psi)$ is the safety factor of the magnetic surface we intend to represent by the invariant curve [31], [33].

We choose a monotonic safety factor profile similar to the one used before in Sections III-B and III-C expressed in terms of the function ψ [31]

$$q(\psi) = \begin{cases} q_0 + c_1\psi + c_2\psi^2, & \psi \le \psi_{95} \\ \alpha \ln(\psi_S - \psi) + \beta, & \psi > \psi_{95}. \end{cases}$$

In the numerical examples, we choose the safety factor parameters, such that the equilibrium magnetic shear at the reference surface, defined as

$$\hat{s}_{95} = \frac{r_{95}}{q_{95}} \frac{dq}{dr}\bigg|_{r_{95}} \tag{15}$$

is $\hat{s}_{95} = 110.8$ and $q_{95} = 3.3$.

For each line, the value of ψ is given by $\psi = \psi(x_0, y_0)$. At each point (x_0, y_0), ψ determines the Δ value

$$\Delta = \Delta(\psi). \tag{16}$$

The map gives the Poincaré map on the surface $\varphi = 0$

$$M_\Delta(x_n, y_n) = (x_{n+1}, y_{n+1}). \tag{17}$$

The magnetic surfaces are shown in Fig. 9.

To perturb the divertor integrable map, we apply the symplectic Martin–Taylor map [26] that simulates the effect of an ergodic limiter in large aspect-ratio tokamaks, which introduces external symmetry-breaking resonances, to generate a chaotic region near the separatrix passing through the X-point.

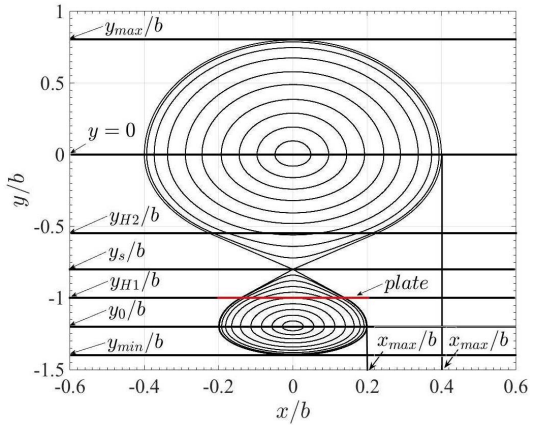

Fig. 9. (Color online) Invariant magnetic surfaces obtained from the integrable map for the chosen parameters indicated in the text.

For each toroidal turn, the Martin–Taylor map is applied at the $\varphi = 0$ surface as a kick perturbation

$$(x^*, y^*) = M_{\Delta_n}(x_n, y_n) \tag{18}$$

$$(x_{n+1}, y_{n+1}) = P(x^*, y^*). \tag{19}$$

Thus, the map used to describe the perturbation of an external resonant helical perturbation due to a magnetic limiter is given by [26]

$$x_{n+1} = x_n - me^{-\frac{my_n}{r_m}} \cos\left(\frac{mx_n}{r_m}\right) \tag{20}$$

$$y_{n+1} = y_n + \frac{r_m}{m} \log\left\{\cos\left[\frac{mx_n}{r_m} - me^{-\frac{mx_n}{r_m}} \cos\left(\frac{mx_n}{r_m}\right)\right]\right\} - \frac{r_m}{m} \log\left\{\cos\left(\frac{mx_n}{r_m}\right)\right\} \tag{21}$$

where the parameter m quantifies the perturbation strength, proportional to the current in the limiter coils, s is the magnetic shear at the plasma edge, and r_m is the plasma radius. The composed field line map is used to obtain the perturbed field line configurations, as shown in Fig. 10, with different magnetic shear profiles at the plasma edge for the control parameters $s = 1.9$ and $s = 2.5$ for $m = 3$. The current in the ergodic limiter is the same in Fig. 10(a) and (b).

The introduced nonaxisymmetric stationary magnetic perturbation leads to the formation of homoclinic tangles near the divertor magnetic saddle [18]. These tangles intersect the divertor plates in static helical structures.

In Fig. 10, we see that the size of the chaotic area near the hyperbolic point depends on the magnetic shear. This dependence is shown in Fig. 11, where we present the chaotic width, the distance from the hyperbolic point to the border of the chaotic region (computed at $y = y_s$) as a function of the parameter s in the interval $1.5 < s < 2.8$, for two different m values. The chaotic area increase should correspond to higher average diffusion time for magnetic field lines to cross the chaotic region. The width increase is not monotonic due to a series of bifurcations that occurs for increasing shear.

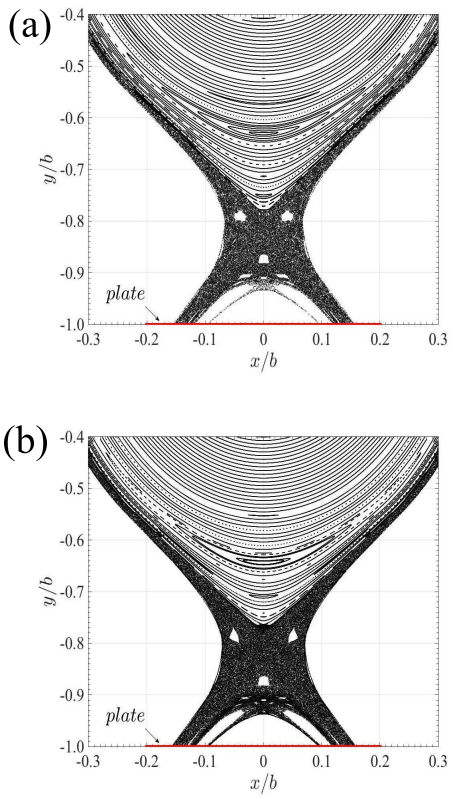

Fig. 10. (Color online) Phase portrait for the total field line map. (a) $s = 1.9$ and $m = 3$. (b) $s = 2.5$ and $m = 3$.

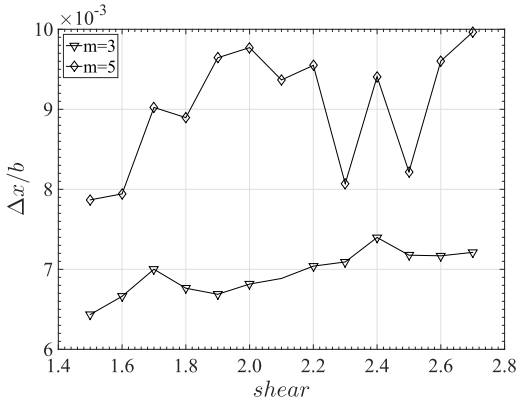

Fig. 11. Normalized width of chaotic area as a function of the magnetic shear s, for $m = 3$ and $m = 5$ and the same parameters of Fig. 10.

V. Conclusion

To describe Poincaré sections of diverted magnetic field lines, we presented 2-D symplectic maps, in the limit of large aspect ratio simulating the alterations, the magnetic topology caused by the divertor.

These maps can be used to investigate the main characteristics of the chaotic layer around the hyperbolic point introduced by divertors, and how these characteristics change with the equilibrium and perturbation control parameters. The tokamap and the Ullmann map were presented in new versions for tokamaks with the divertor. We also presented a map describing magnetic surfaces in toroidal geometry.

All the maps introduced in this paper are useful for studying different aspects of the field line dynamics and transport in tokamaks with the divertor. Extensions of the presented maps could be derived to include additional effects not considered in this paper, such as the particle's finite Larmor radius [34], [35] and the screening caused by the plasma response to resonant magnetic perturbations [36], [37].

References

[1] C. W. Horton, Jr., and S. Benkadda, *ITER Physics*, 1nd ed. Singapore: World Scientific, 2015, p. 248.
[2] C. W. Horton, *Turbulent Transport in Magnetized Plasmas*, 1st ed. NJ, USA: World Scientific, 2012, p. 520.
[3] R. D. Hazeltine and J. D. Meiss, *Plasma Confinement*, 1nd ed. New York, NY, USA: Dover, 2003, p. 480.
[4] F. Karger and K. Lackner, "Resonant helical divertor," *Phys. Lett. A*, vol. 61, pp. 385–387, Jun. 1977.
[5] F. Wagner *et al.*, "Regime of improved confinement and high beta in neutral-beam-heated divertor discharges of the ASDEX tokamak," *Phys. Rev. Lett.*, vol. 49, no. 19, pp. 1408–1414, Nov. 1982.
[6] M. Kikuchi, K. Lackner, M. Q. Tran, *Fusion Physics*, 1st ed. Vienna, AT, USA: IAEA, 2012, p. 1129.
[7] ITER Physics Expert Group on Divertor, "Power and particle control," in *Nuclear Fusion*, vol. 39. Vienna, Austria: Nuclear Fusion IAEA, 1999, ch. 4, pp. 2391–2469.
[8] T. E. Evans, R. A. Moyer, and P. Monat, "Modeling of stochastic magnetic flux loss from the edge of a poloidally diverted tokamak," *Phys. Plasmas*, vol. 9, pp. 4957–4967, Nov. 2002.
[9] E. C. da Silva, I. L. Caldas, R. L. Viana, and M. A. F. Sanjuán, "Escape patterns, magnetic footprints, and homoclinic tangles due to ergodic magnetic limiters," *Phys. Plasmas*, vol. 9, pp. 4917–4928, Nov. 2002.
[10] P. J. Morrison, "Magnetic field lines, Hamiltonian dynamics, and nontwist systems," *Phys. Plasmas*, vol. 7, pp. 2279–2289, May 2000.
[11] S. S. Abdullaev, *Construction of Mappings for Hamiltonian Systems and Their Applications*, vol. 691. 2nd ed. Berlin, Germany: Springer-Verlag, 2006, p. 379.
[12] J. S. E. Portela, I. L. Caldas, and R. L. Viana, "Tokamak magnetic field lines described by simple maps," *Eur. Phys. J. Special Topics*, vol. 165, pp. 195–210, Dec. 2008.
[13] I. L. Caldas *et al.*, "Control of chaotic magnetic fields in tokamaks," *Braz. J. Phys.*, vol. 32, no. 4, pp. 980–1004, Dec. 2002.
[14] S. R. Barocio, E. Chávez-Alarcón, C. Gutierrez-Tapia, "Mapping the intrinsic stochasticity of tokamak divertor configuration," *Brazilian J. Phys.*, vol. 36, no. 2B, pp. 550–556, Jun. 2006.
[15] D. Ciro, T. E. Evans, and I. L. Caldas, "Modeling non-stationary, non-axisymmetric heat patterns in DIII-D tokamak," *Nucl. Fusion*, vol. 57, no. 1, p. 016017, 2017.
[16] C. G. L. Martins, M. Roberto, and I. L. Caldas, "Delineating the magnetic field line escape pattern and stickiness in a poloidally diverted tokamak," *Phys. Plasmas*, vol. 21, no. 8, p. 082506, Jul. 2014.
[17] A. Vannucci, I. L. Caldas, and I. C. Nascimento, "Disruptive instabilities in the discharges of the TBR-1 small tokamak," *Plasma Phys. Control. Fusion*, vol. 31, no. 2, p. 147, Feb. 1989.
[18] A. Wingen, T. E. Evans, and K. H. Spatschek, "High resolution numerical studies of separatrix splitting due to non-axisymmetric perturbation in DIII-D," *Nucl. Fusion*, vol. 49, no. 5, p. 055027, Apr. 2009.
[19] J. D. Meiss, "Symplectic maps, variational principles, and transport," *Rev. Mod. Phys.*, vol. 64, no. 3, pp. 795–848, Jul. 1992.
[20] J. M. Greene, "A method for determining a stochastic transition," *J. Math. Phys.*, vol. 20, no. 6, pp. 1183–1201, Jun. 1979.
[21] B. V. Chirikov, "A universal instability of many-dimensional oscillator systems," *Phys. Rep.*, vol. 52, no. 5, pp. 263–379, May 1979.
[22] M. D. Kruskal, "Some properties of rotational transforms," Princeton Univ. Forrestal Res. Center, Princeton, NJ, USA, Project Matterhorn Rep. NY0-998, PM-S-5, 1952
[23] C. W. Horton, H.-B. Park, J.-M. Kwon, D. Strozzi, P. J. Morrison, and D.-I. Choi, "Drift wave test particle transport in reversed shear profile," *Phys. Plasmas*, vol. 5, no. 11, pp. 3910–3917, Nov. 1998.
[24] D. del-Castillo-Negrete and P. J. Morrison, "Chaotic transport by Rossby waves in shear flow," *Phys. Fluids A*, vol. 5, no. 4, pp. 948–965, Apr. 1993.
[25] D. del-Castillo-Negrete, J. Greene, and P. J. Morrison, "Area preserving nontwist maps: Periodic orbits and transition to chaos," *Physica D*, vol. 91, pp. 1–23, Mar. 1996.

[26] T. J. Martin and J. B. Taylor, "Ergodic behaviour in a magnetic limiter," *Plasma Phys. Control. Fusion*, vol. 26, pp. 321–340, Mar. 1984.
[27] A. Punjabi, A. Verma, and A. Boozer, "Stochastic broadening of the separatrix of a tokamak divertor," *Phys. Rev. Lett.*, vol. 69, no. 23, pp. 3322–3325, Dec. 1992.
[28] R. Balescu, M. Vlad, and F. Spineanu, "Tokamap: A Hamiltonian twist map for magnetic field lines in a toroidal geometry," *Phys. Rev. E, Stat. Phys. Plasmas Fluids Relat. Interdiscip. Top.*, vol. 58, pp. 951–964, Jul. 1998.
[29] K. Ullmann and I. L. Caldas, "A symplectic mapping for the ergodic magnetic limiter and its dynamical analysis," *Chaos, Solitons Fractals*, vol. 11, no. 13, pp. 2129–2140, Oct. 2000.
[30] Ph. Ghendrih, A. Grosman, and H. Capes, "Theoretical and experimental investigations of stochastic boundaries in tokamaks," *Plasma Phys. Control. Fusion*, vol. 38, no. 10, pp. 1653–1724, 1996.
[31] T. Kroetz, M. Roberto, I. L. Caldas, R. L. Viana, and P. J. Morrison, "Divertor map with freedom of geometry and safety factor profile," *Plasma Phys. Control Fusion*, vol. 54, no. 4, p. 045007, Mar. 2012.
[32] T. Kroetz, M. Roberto, I. L. Caldas, R. L. Viana, P. J. Morrison, and P. Abbamonte, "Integrable maps with non-trivial topology: Application to divertor configurations," *Nucl. Fusion*, vol. 51, no. 034003, Feb. 2010.
[33] G. Roberson, M. Roberto, I. L. Caldas, T. Kroetz, and R. L. Viana, "Shaping diverted plasmas with symplectic maps," *IEEE Trans. Plasma Phys.*, vol. 45, no. 3, pp. 356–363, Feb. 2017.
[34] J. J. Martinell and D. del-Castillo-Negrete, "Gyroaverage effects on chaotic transport by drift waves in zonal flows," *Phys. Plasmas*, vol. 20, no. 022303, Feb. 2013.
[35] J. D. da Fonseca, D. del-Castillo-Negrete, and I. L. Caldas, "Area-preserving maps models of gyroaveraged E×B chaotic transport," *Phys. Plasmas*, vol. 21, p. 092310, Sep. 2014.
[36] A. Wingen *et al.*, "Connection between plasma response and resonant magnetic perturbation (RMP) edge localized mode (ELM) suppression in DIII-D," *Plasma Phys. Control. Fusion*, vol. 57, no. 10, p. 104006, Sep. 2015.
[37] A. C. Fraile, Jr., M. Roberto, I. L. Caldas, and C. G. L. Martins, "Plasma response to resonant magnetic perturbations in large aspect ratio tokamaks," *IEEE Trans. Plasma Sci.*, vol. 45, no. 11, pp. 2906–2912, Oct. 2017.

Iberê Luiz Caldas was born in Santos, Brazil, in 1948. He received the B.S. and Ph.D. degrees in physics from the Institute of Physics, University of São Paulo (IF-USP), São Paulo, Brazil, in 1970 and 1979, respectively.

In 1977–1979, 1983, 1984, and 1988, he was a Guest Scientist with the Max-Planck-Institut für Plasmaphysik, Garching bei München, Germany. Since 1995, he has been a Full Professor with IF-USP. His current research interests include plasma physics and chaos.

Bruno F. Bartoloni received the Ph.D. degree in plasma physics from the Institute of Physics, Universidade de São Paulo, São Paulo, Brazil, in 2016.

He has been a Professor with the Physics Department, Faculdade de Tecnologia de São Paulo, São Paulo, since 2017. His current research interests include different current density profiles applied in symplectic maps to study the magnetic field lines in a plasma confined in a tokamak.

David Ciro received the B.S. degree from the University of Antioquia, Medellín, Colombia, USA, in 2010, and the M.Sc. and Ph.D. degrees from the Universidade de São Paulo, São Paulo, Brazil, in 2012 and 2016, respectively, all in physics.

In 2015, he was a Visiting Researcher with the DIII-D Facilities, General Atomics, San Diego, CA, USA. He is currently a Post-Doctoral Researcher of nonlinear dynamics applied to plasma physics with the Department of Physics, Federal University of Paraná, Curitiba, Brazil.

Geraldo Roberson received the B.Sc. degree in physics from the Federal University of Pernambuco, Recife, Brazil, and the M.Sc. degree in plasma physics from the Aeronautics Institute of Technology, São José dos Campos, Brazil, where he is currently pursuing the Ph.D. degree in sciences and space technologies.

Adriane B. Schelin received the Ph.D. degree in physics from the Institute of Physics, University of São Paulo, São Paulo, Brazil, in 2009.

From 2009 to 2010, she was a Visiting Researcher with the Heinrich-Heine-Universität Düsseldorf, Düsseldorf, Germany. In 2011 and 2012, she was a Professor with the Physics Academic Department, Universidade Tecnológica Federal do Paraná, Curitiba, Brazil. She has been a Professor with the Institute of Physics, University of Brasília, Brasilia, Brazil, since 2013.

Tiago Kroetz received the Ph.D. degree in plasma physics from the Instituto Tecnolgico de Aeronáutica, São José dos Campos, Brazil, in 2010.

Since 2010, he has been involved in research about nonlinear dynamics applied to plasma physics and mechanical systems, and also extended to the field of research on the physics education. He has been a Professor with the Physics Academic Department, Federal Technological University of Paraná, Pato Branco, Brazil, since 2012.

Marisa Roberto received the B.S. degree in physics from the Catholic University of São Paulo, São Paulo, Brazil, in 1982, the M.S. degree from the Space Research Institute, São José dos Campos, Brazil, in 1986, and the Ph.D. degree in plasma physics from the Aeronautics Institute of Technology (ITA), São José dos Campos, in 1992.

In 1999 and 2004, she was a Visiting Scholar with the University of California at Berkeley, Berkeley, CA, USA. She is currently a Full Professor with the Physics Department, ITA. Her current research interests include plasma physics for technological applications and chaos.

Ricardo Luiz Viana received the Ph.D. degree in plasma physics from the Institute of Physics, Universidade de São Paulo, São Paulo, Brazil, in 1991.

In 1987, he was a Visiting Scholar with the Institute for Physical Science and Technology, University of Maryland, College Park, MD, USA. He has been a Professor with the Physics Department, Federal University of Paraná, Curitiba, Brazil, since 1989. He has authored 190 papers and supervised 10 doctoral theses, and 3 post-doctoral works.

Kelly Cristiane Iarosz received the Ph.D. degree in science/physics from the State University of Ponta Grossa, Ponta Grossa, Brazil, in 2013.

In 2014, she was a Visiting Researcher with the Institute for Complex Systems and Mathematical Biology, Aberdeen University, Aberdeen, U.K., where she has been an Honorary Researcher since 2015. In 2017, she was an Academic Visitor with the Institute of Complex Systems and Control, Xi'an University of Technology, Xi'an, China. She is a Visiting Researcher with Humboldt-Universität zu Berlin, Berlin, Germany, and the Potsdam Institute for Climate Impact Research, Potsdam, Germany. She is currently a Post-Doctoral Researcher with the Institute of Physics, São Paulo University.

Antonio Marcos Batista received the Ph.D. degree in physics from the Federal University of Paraná, Curitiba, Brazil, in 2001.

From 2014 to 2015, he was a Visiting Researcher with the Institute for Complex Systems and Mathematical Biology, Aberdeen University, Aberdeen, U.K., where he has been an Honorary Researcher since 2015. He was a Visiting Scholar with the Potsdam Institute for Climate Impact Research, Potsdam, Germany, in 2016, and the Xi'an University of Technology, China, in 2017. He has been an Associate Professor with the Mathematics and Statistics Department, State University of Ponta Grossa, Ponta Grossa, Brazil, since 1997.

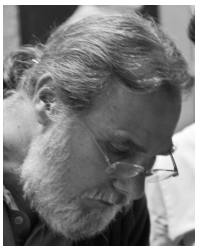

Philip J. Morrison has investigated the nonlinear Hamiltonian dynamics of few and infinite degree-of-freedom systems for many years. As a member of the Institute for Fusion Studies, The University of Texas at Austin, Austin, TX, USA, he has been involved in basic and applied plasma physics problems. He has been associated with the Geophysical Fluid Dynamics Program for 20 years, and as a member of its faculty, he is involved in basic and applied fluid mechanics problems. He has also been involved in developing and applying advanced computational algorithms, in part through affiliation with the ICES Applied Mathematics Group, University of Texas at Austin. He is a Mathematical and Theoretical Physicist with broad interests.